Adaptive Internal Model Theory of the Oculomotor System and the Cerebellum

Mireille E. Broucke

***Abstract*—We present a computational model of the oculomotor system and the cerebellum. In contrast with prevailing theories of cerebellar function, we propose the cerebellum embodies adaptive internal models of all persistent, exogenous, deterministic signals acting on the body and observable through the error signals it receives. Our model is validated by simulations, recovering results from a number of oculomotor experiments.**

I. Introduction

This paper presents a control-theoretic model of the oculomotor system and the cerebellum. We show that developments on adaptive internal models [34], [35], [39], [48], [49], [53], [57] provide a compelling framework to explain the overall system. We obtain a model that is extremely simple, yet is able to explain more behaviors than previous models. In addition, we make a proposal on the function of the cerebellum: the cerebellum embodies adaptive internal models of persistent, exogenous, deterministic signals observable through the error signals it receives.

Since the 1960's with the pioneering work of D.A. Robinson, control-theoretic models have provided a powerful tool to explain the oculomotor system [45]; these include models of the optokinetic system, the saccadic system, the smooth pursuit system, gaze holding, and the vestibulo-ocular reflex (VOR), among others; see [14], [41], [59] for overviews. Despite impressive advances, these models tend to be fragmented, with one model explaining gaze holding but not smooth pursuit, another explaining smooth pursuit but not the VOR, and so forth. The idea that there can be a unifying principle underlying all these models is currently not developed. Certain behaviors such as the so-called predictive capability of the oculomotor system are not yet fully understood, and the computations of the cerebellum are often excluded.

Since the 1990's neuroscientists have explored internal models as a means to explain the function of the cerebellum [21], [22], [36], [55]. These internal models of neuroscience correspond to models of the open-loop plant (for instance, the arm or the leg or the eye). We have found that in all cases, neuroscientists use the term "internal model" in a sense that is distinct from the internal model principle of control theory [11]. The idea that the cerebellum may be involved in generating internal models of disturbance signals has been suggested based on experimental evidence in [7], [8], [29], but a computational model that includes the internal model principle has not been presented before.

We summarize our contributions as follows. (i) We present a comprehensive mathematical model of the slow eye movement subsystems of the oculomotor system, replicating a number of oculomotor experiments. We are not aware of any computational model that collectively explains these behaviors. (ii) Our model formalizes a hypothesis that the function of the cerebellum is to provide internal models of persistent, exogenous, deterministic signals acting on a biological system. This contrasts with prevailing theories that the cerebellum embodies forward and inverse models of the plant [22], [42]. (iii) We show that adaptive internal models [34], [35], [39], [48], [49], [53], [57] provide an ideal starting point to develop this computational model in the sense that almost no adjustments to current theoretical frameworks for adaptive internal models are needed.

This paper is a companion to [4]. In this paper we derive the model, prove its correctness, discuss the neural circuit, and present simulations focusing on neurological and lesion experiments. In [4] we present complementary simulations focusing on behavioral experiments.

II. Control Architecture

The proposed control architecture is shown in Figure 1 and is based on the neural circuit of the oculomotor system [27]. A visual error signal encoding the difference between target and gaze angles is transmitted from the *visual cortex* to the *inferior olive* (IO), where it is relayed to appropriate *climbing fiber* inputs (CFs) of the *cerebellum* (C) (specifically, the *floccular complex*). The cerebellum also receives *mossy fiber* inputs (MFs) containing a mixture of visual, eye movement, and vestibular information from the *medial vestibular nuclei* (MVN) in the *brainstem* (B) [29]. The sole output of the cerebellum is transmitted via its *Purkinje cells* (PCs) to *floccular target neurons* (FTNs) in the MVN [43]. The MVN also receives a head velocity signal from the semicircular canals of the ear. The output of the MVN is sent both to the *neural integrator* (NI) in the brainstem *nucleus prepositus hypoglossi* (NPH) and directly to the *oculomotor neurons* (MNs) of the oculomotor plant (P). Salient features of this architecture include: (i) the cerebellum forms a side loop to the main feedback loop between the plant and the brainstem; (ii) the brainstem has a direct feedthrough from the vestibular system to the plant to cancel measurable disturbance signals from head movement; (iii) the CF cerebellar input is a sensory error signal carrying visual information; and (iv) the cerebellum has only one output which acts as a top up to the control command generated by a brainstem-only pathway. Our aim is to develop a model that abides by this architecture.

III. Oculomotor Plant and Brainstem

The horizontal motion of the eye is modeled by considering the eyeball as a sphere that is suspended in fluid and subjected to viscous drag, elastic restoring forces, and the pulling of two muscles. A reasonable approximation is obtained by assuming

The author is with the Dept. of Electrical and Computer Engineering, University of Toronto, Canada (e-mail: broucke@control.utoronto.ca). Supported by the Natural Sciences and Engineering Research Council of Canada (NSERC).

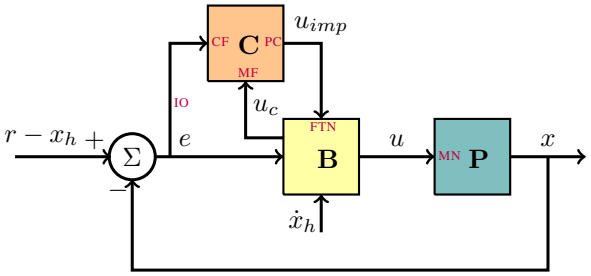

Fig. 1: Control architecture for the oculomotor system.

that the inertia of the eyeball is insignificant [27], [45], [52]. Letting x be the horizontal eye angle and u be the net torque imparted by the two muscles, we obtain a first order model

$$\dot{x} = -K_x x + u\,. \tag{1}$$

The parameter $K_x > 0$ is constant (or very slowly varying) such that the time constant of the eye is $\tau_x := 1/K_x \simeq 0.2$s [45]. This first order model may be compared with the model of an ocular motoneuron. Let f be the firing rate, and let f_0 be the baseline firing rate when the eye is stationary at $x = 0$. A commonly used model of neuronal firing rate is $f = f_0 + c_1 x + c_2 \dot{x}$, where c_1 and $c_2 \neq 0$ are constants [45], [52]. Comparing this model with (1), we observe $K_x = c_1/c_2$ and $u = \frac{1}{c_2}(f - f_0)$. That is, the torque is proportional to the firing rate, modulo a constant offset of f_0.

Next consider a reference signal r representing the angle of a target moving in the horizontal plane. Let x_h and $\dot{x}_h$ denote the horizontal head angular position and angular velocity, respectively. The *retinal error* is defined to be

$$e := \alpha_e(r - x_h - x)\,. \tag{2}$$

Notice that $r - x_h - x$ is the target angle r relative to the *gaze angle* $x_h + x$. For sufficiently distant targets, this relative angle is proportional (through the scale factor $\alpha_e \in \mathbb{R}$) to a linear displacement on the retina from the fovea to the target. Since the goal of the oculomotor system is to drive e to zero, for the purposes of the present paper we set $\alpha_e = 1$.

Our modeling assumptions are as follows. The eye position x is assumed to be unavailable for direct measurement [18]. The retinal error signal e (or a scaled version of it) is assumed to be available as a measurement to the brainstem and to both MF and CF inputs of the cerebellum [2], [25]. The reference signal r is unmeasurable. The vestibular system provides a measurement of the head angular velocity $\dot{x}_h$ to the brainstem but not directly to the cerebellum [13], [45], and it does not provide the head position x_h [45].

To model the brainstem, we start from Robinson's parallel pathway model [51] consisting of two parallel pathways that combine to form the motor command; that is, $u = u_v + u_n$, where u_v is carried on the direct pathway from the MVN to the MNs; and u_n corresponds to an indirect pathway from MVN to NPH to MNs. The signal u_n is the output of the *brainstem neural integrator* in the NPH. Invoking equation (3) in [44], the neural integrator is modeled as a leaky integrator:

$$\dot{\hat{x}} = -\widetilde{K}_x \hat{x} + u_v\,, \quad u_n = \alpha_x \hat{x}\,, \tag{3}$$

where α_x and $\widetilde{K}_x$ are constants (or very slowly varying). Using the fact that $u_v = u - \alpha_x \hat{x}$, this model can be re-expressed as

$$\dot{\hat{x}} = -\widehat{K}_x \hat{x} + u\,, \tag{4}$$

where $\widehat{K}_x := \widetilde{K}_x + \alpha_x$. Finally, we incorporate the idea from [12] that $\widehat{K}_x = K_x$ (henceforth we drop the hat); see also [9], [16]. In sum, we deduce that the brainstem neural integrator forms an *observer* of the oculomotor plant. If we define the estimation error $\widetilde{x} := x - \hat{x}$, then $\widetilde{x}$ evolves according to $\dot{\widetilde{x}} = -K_x \widetilde{x}$, implying that $\hat{x}(t)$ converges exponentially to $x(t)$. Aside from a momentary perturbation (a push on the eyeball), $\hat{x}(t)$ well approximates $x(t)$.

Remark 3.1: The major variants of the brainstem model can be derived from (3). When $\hat{K}_x = K_x$, the model is called a *forward model* in the neuroscience literature. With the choice $\widehat{K}_x = 0$ and $\alpha_x = K_x$, the model is called an *inverse model*, because it cancels the stable pole of the oculomotor plant. The inverse model is not accurate since the neural integrator is leaky [44]; nevertheless, it finds use in models of the saccadic system [41] to allow modelers to account for gaze holding at the end of a saccade without explicitly modeling the contribution from the cerebellum. Namely, the inverse model inserts a pole at zero to allow the eye to track an exosystem $R(s) = 1/s$. ◁

Remark 3.2: Our assumption that $\widehat{K}_x = K_x$ implicitly relies on the existence of two additional brain processes. First we assume that the brain is capable of *long-term adaptation* (over days and weeks) to changes in model parameters (e.g. weakening of the muscles of the eye) [27]. Second, we assume the brain is capable of *learning transfer*, a process by which adapted parameter values can be transferred from one brain region to another (cerebellum to brainstem) [19], [50]. ◁

As a final step in modeling the brainstem, we consider the components of the signal u_v. In our model there are three: $u_v = u_s + u_{imp} - \alpha_h \dot{x}_h$. The signal $\alpha_h \dot{x}_h$ is the vestibular measurement of head angular velocity representing the direct feedthrough from the semicircular canals to the MNs; the signal u_s carries visual information; and the signal u_{imp} is the output from the PCs of the cerebellum.

IV. Disturbance Rejection Problem

We approach the derivation of a model of the cerebellum as a problem of control synthesis: to design a controller to drive the error e to zero. To this end, we depart from biologically relevant signals, and we instead use mathematical variables in order to distinguish disturbances that are cancelled in the brainstem from disturbances that must be rejected by the cerebellum. In particular, we define the brainstem-only signal

$$u_b = \alpha_x \hat{x} - \alpha_h \dot{x}_h\,. \tag{5}$$

Also let $u_c = u_s + u_{imp}$. Then $u = u_v + u_n = u_b + u_c$. Assuming that $\hat{x}(t) \simeq x(t)$ for $t \geq 0$, we obtain the *error model*

$$\dot{e} = -\widetilde{K}_x e - u_c + \dot{r} + \widetilde{K}_x r - (1 - \alpha_h)\dot{x}_h - \widetilde{K}_x x_h\,, \tag{6}$$

where $\widetilde{K}_x := K_x - \alpha_x$.

We assume that the reference signal r as well as the head position x_h are modeled as the outputs of a linear exosystem. Let $\eta \in \mathbb{R}^q$ be the exosystem state and define the exosystem $\dot{\eta} = S\eta$, $r = D_1\eta$, $x_h = D_2\eta$, where $S \in \mathbb{R}^{q\times q}$, $D_1 \in \mathbb{R}^{1\times q}$, and $D_2 \in \mathbb{R}^{1\times q}$. Then (6) takes the form

$$\dot{e} = -\widetilde{K}_x e - u_c + E\eta \tag{7}$$

where $E := D_1 S + \widetilde{K}_x D_1 - (1-\alpha_h)D_2 S - \widetilde{K}_x D_2 \in \mathbb{R}^{1\times q}$.

It is useful to transform the exosystem using the technique in [38]. Let (F, G) be a controllable pair with F Hurwitz. Define the coordinate transformation $w = M\eta$, with $M \in \mathbb{R}^{q\times q}$ nonsingular and satisfying the Sylvester equation $MS = FM + GE$ (w.l.o.g. we assume (E, S) is observable and the spectra of S and F are disjoint) [38]. Also define $\Psi := EM^{-1} \in \mathbb{R}^{1\times q}$. In new coordinates, the exosystem model is $\dot{w} = (F + G\Psi)w$. Because $E\eta = \Psi w$, we can write the error dynamics (7) in terms of the new exosystem state:

$$\dot{e} = -\widetilde{K}_x e - u_c + \Psi w\,. \tag{8}$$

The parameters $(\widetilde{K}_x, \Psi^{\mathrm{T}}) \in \mathbb{R}^{q+1}$ capture all unknown model and disturbance parameters.

Problem 4.1: Consider the error model (8). Suppose the unknown parameters $(\widetilde{K}_x, \Psi^{\mathrm{T}})$ belong to a known compact set $\mathcal{P} \subset \mathbb{R}^{q+1}$. Find an error feedback compensator such that for all closed-loop initial conditions and all $(\widetilde{K}_x, \Psi^{\mathrm{T}}) \in \mathcal{P}$, $\lim_{t\to\infty} e(t) = 0$. ◁

V. Cerebellum

Our model of the cerebellum takes the form of an *adaptive internal model* consisting of an internal model of the disturbances impinging on the retinal error combined with a parameter estimation process to recover the unknown parameters [48]. Let $\hat{w}$ and $\hat{\Psi}$ be estimates of w and Ψ, respectively. The controller is

$$\dot{\hat{w}} = F\hat{w} + Gu_c \tag{9}$$

$$u_c = u_{imp} + u_s\,. \tag{10}$$

The feedback u_s is selected to make the closed-loop system asymptotically stable. We choose $u_s = K_e e$, with $K_e > 0$ sufficiently large. We choose $u_{imp} = \hat{\Psi}\hat{w}$, where $\hat{\Psi}$ is an estimate of Ψ. If $\hat{\Psi} = \Psi$, then the internal model has the form

$$\dot{\hat{w}} = (F + G\Psi)\hat{w} + GK_e e\,,$$

so it includes the unstable poles of the exosystem, thus satisfying the internal model principle. Based on a Lyapunov argument, the adaptation law for the parameter estimate is $\dot{\hat{\Psi}} = e\hat{w}^{\mathrm{T}}$. The overall design is

$$\dot{\hat{x}} = -K_x\hat{x} + u \tag{11a}$$

$$\dot{\hat{w}} = F\hat{w} + Gu_c \tag{11b}$$

$$\dot{\hat{\Psi}} = e\hat{w}^{\mathrm{T}} \tag{11c}$$

$$u_b = \alpha_x\hat{x} - \alpha_h\dot{x}_h \tag{11d}$$

$$u_c = \hat{\Psi}\hat{w} + K_e e \tag{11e}$$

$$u = u_b + u_c\,. \tag{11f}$$

Theorem 5.1: Consider the closed-loop system (8) and (11), where $K_x > 0$ and F is Hurwitz. Suppose the unknown parameters $(\widetilde{K}_x, \Psi^{\mathrm{T}})$ belong to a known compact set $\mathcal{P} \subset \mathbb{R}^{q+1}$. Then there exists $K_e > 0$ sufficiently large such that for all initial conditions $(e(0), w(0), \hat{w}(0), \widetilde{x}(0), \hat{\Psi}(0))$ and for all $(\widetilde{K}_x, \Psi^{\mathrm{T}}) \in \mathcal{P}$, the solution satisfies $\lim_{t\to\infty} e(t) = 0$.

Proof: The proof is based on [48]. Define the estimation errors: $\widetilde{x} = x - \hat{x}$, $\widetilde{w} := \hat{w} - w + Ge$, and $\widetilde{\Psi} := \hat{\Psi} - \Psi$. In terms of these errors we have

$$\dot{e} = -Ke + \alpha_x\widetilde{x} - \Psi\widetilde{w} - \widetilde{\Psi}\hat{w} \tag{12a}$$

$$\dot{\widetilde{w}} = F\widetilde{w} - He + \alpha_x G\widetilde{x} \tag{12b}$$

$$\dot{\widetilde{x}} = -K_x\widetilde{x}\,, \tag{12c}$$

where $K := K_x - \alpha_x + K_e - \Psi G$ and $H := FG + G\widetilde{K}_x$. Suppose that $\widetilde{\Psi} = 0$ in (12), and let $\widetilde{\xi} := (\widetilde{w}, \widetilde{x})$. Then (12) becomes

$$\dot{e} = -Ke + \widetilde{G}\widetilde{\xi} \tag{13a}$$

$$\dot{\widetilde{\xi}} = \widetilde{F}\widetilde{\xi} + \widetilde{H}e \tag{13b}$$

where $\widetilde{F} = \begin{bmatrix} F & \alpha_x G \\ 0 & -K_x \end{bmatrix}$, $\widetilde{G} = \begin{bmatrix} -\Psi & \alpha_x \end{bmatrix}$, and $\widetilde{H} = \begin{bmatrix} -H \\ 0 \end{bmatrix}$. By assumption F is Hurwitz and $K_x > 0$, so $\widetilde{F}$ is Hurwitz. Given any $\gamma > 0$, there exists a symmetric, positive definite matrix $P \in \mathbb{R}^{(q+1)\times(q+1)}$ such that $P\widetilde{F} + \widetilde{F}^{\mathrm{T}}P = -\gamma I$. Define the Lyapunov function $V := \|e\|^2 + \widetilde{\xi}^{\mathrm{T}}P\widetilde{\xi}$. The derivative of V along solutions of (13) is

$$\begin{aligned} \dot{V}_{(13)} &= -2K\|e\|^2 + 2e\widetilde{G}\widetilde{\xi} + 2\widetilde{\xi}^{\mathrm{T}}P\widetilde{H}e - \gamma\|\widetilde{\xi}\|^2 \\ &= \begin{bmatrix} e^{\mathrm{T}} & \widetilde{\xi}^{\mathrm{T}} \end{bmatrix} \begin{bmatrix} -2K & \widetilde{G} + \widetilde{H}^{\mathrm{T}}P \\ \widetilde{G}^{\mathrm{T}} + P\widetilde{H} & -\gamma I \end{bmatrix} \begin{bmatrix} e \\ \widetilde{\xi} \end{bmatrix}. \end{aligned}$$

Since the unknown parameters $(\widetilde{K}_x, \Psi^{\mathrm{T}})$ belong to a compact set $\mathcal{P}$, the off-diagonal elements of the matrix above are bounded. Then by a standard argument we can choose $K > 0$ sufficiently large (by choosing $K_e > 0$ sufficiently large) such that the matrix is negative definite for all $(\widetilde{K}_x, \Psi^{\mathrm{T}}) \in \mathcal{P}$.

Now consider (12) with $\widetilde{\Psi} \neq 0$ and define the Lyapunov function $V_\Psi := V + \widetilde{\Psi}\widetilde{\Psi}^{\mathrm{T}}$. Using (11c), the derivative of V_Ψ along solutions of (12) is $\dot{V}_\Psi = \dot{V}_{(13)} - 2e\widetilde{\Psi}\hat{w} + 2\widetilde{\Psi}\dot{\widetilde{\Psi}}^{\mathrm{T}} = \dot{V}_{(13)} \leq 0$. Finally, applying the LaSalle Invariance Principle, we obtain that $\lim_{t\to\infty} e(t) = 0$, as required. ■

VI. Simulations

We validated our model using simulations of experiments with the slow eye movement systems; see also [3], [4]. The parameter values for the simulations are: $K_x = 5$, $\alpha_x = 0.95K_x$, $\alpha_h = 0.65$, $K_e = 5$, $q = 2$, $F = \begin{bmatrix} 0 & 1 \\ -1 & -1 \end{bmatrix}$, and $G = \begin{bmatrix} 0 \\ 1 \end{bmatrix}$. These values were selected according to the following criteria. First, K_x is selected to match the known time constant $\tau_x = 1/K_x = 0.2$s of the human oculomotor plant. Second, α_x is selected so that $\widetilde{K}_x = K_x - \alpha_x = 0.25$ gives a time constant of $\tilde{\tau}_x = 1/\widetilde{K}_x = 4$s, in the range of the known time constant of the combined oculomotor plant and neural integrator [14]. The final top-up to this time constant is provided by the cerebellum; see the discussion on gaze fixation below. We have chosen α_h called the VOR gain

(see below) somewhat arbitrarily; it may range from 0.6 to 0.9 under natural conditions and is highly adaptable. The parameter $K_e = 5$ has been selected to match the transient response of the smooth pursuit system (see Figure 6); however, it too appears to be adjustable [4]. The parameter q which sets the order of the internal model is of great interest and may vary according to which module of the cerebellum is under study. For the floccular complex, we have selected $q = 2$ based on the performance of the human smooth pursuit system; see Remark 6.1. We have selected F so the adaptive internal model has stable complex conjugate poles. This behavior is clearly evident in the damped oscillations of the smooth pursuit system when initiating tracking of a constant speed target [46].

Vestibulo-Ocular Reflex: The purpose of the vestibulo-ocular reflex (VOR) is to stabilize the gaze (sum of eye and head angles) when the head is moving. This system has been intensively studied over the last 60 years, and experiments may be classified as follows. (a) The standard *behavioral experiment* with the VOR involves involuntary sinusoidal rotation of the subject's head in darkness. The ratio of peak eye velocity to peak head velocity in steady-state is called the *VOR gain*. Another behavioral experiment involves involuntary sinusoidal rotation of the subject's head in the light, while the subject fixates on a stationary target. In this case, the *effective VOR gain* jumps to close to unity in human subjects. (b) *VOR Cancellation* is an experiment in which the subject's head is moved involuntarily while the subject must track a target that moves with the head. The experiment is called VOR cancellation because the brain must suppress its own (brainstem) reflex to move the eyes opposite to the head. (c) *VOR adaptation experiments* involve experimental adaptation of the VOR gain. (d) *Neurological experiments* typically record from the cells of the MVN or the Purkinje cells of the cerebellum. (e) *Lesion experiments* involve total cerebellectomy, lesions of the flocculus only, the MVN, the NPH, or some combination thereof.

First we consider the standard experiment of measuring the VOR gain. This gain is measured in darkness when the cerebellum is relatively inactive, so in our model we assume $u_c = 0$. It can be shown that for a sinusoidal head rotation, the steady-state eye position evolves as $x(t) \simeq -\alpha_h x_h(t)$ [4]. Therefore, in our model the parameter α_h is precisely the VOR gain. Results for the second standard VOR experiment showing that the effective VOR gain in the light is unity are given in [4, Fig. 1]; the cerebellum adapts to different frequencies of sinusoidal head rotation. Results for VOR cancellation showing that the cerebellum is able to cancel the brainstem reflex signal $-\alpha_h \dot{x}_h$ are given in [4, Fig. 3].

Next we consider experiments involving an adapted VOR gain. As discussed in Remark 3.2, the VOR gain α_h is subject to an adaptive brain process called long-term adaptation. While we do not include this process in our model (α_h is treated as a constant), we can consider how an adapted VOR gain affects short-term behavior of the oculomotor system. In [4, Fig. 2] we presented results for an experiment exploring the transient response to a step input of head velocity when the VOR gain α_h has been adapted to values $\alpha_h = 0.3, 0.5, 0.8$ [32]. In a

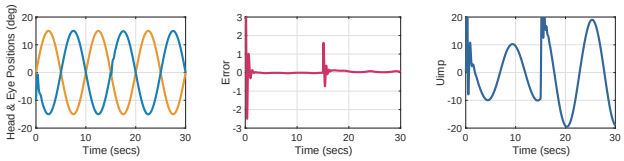

Fig. 2: Effect of α_h on the VOR. From left to right, the head (yellow) and eye (blue) angles, the retinal error e, and the cerebellar component u_{imp}. Notice that the eye position is unaffected by the value of α_h in steady-state.

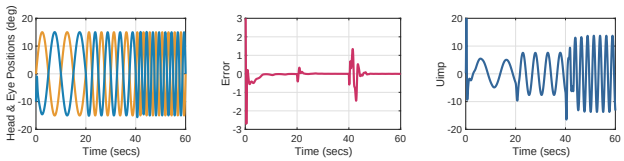

Fig. 3: Effect of the frequency of oscillations of the head on the depth of modulation of the cerebellar component u_{imp}. From left to right, the head (yellow) and eye (blue) angles, the retinal error e, and the cerebellar component u_{imp}. Notice the amplitude of u_{imp} increases as the frequency of oscillation of the head increases.

second experiment documented in [28], monkeys were adapted to a new VOR gain by wearing goggles in their cages. It was found that changes in the VOR gain had no affect on the monkey's ability to track a moving target. This behavior is explained in our model when we consider that the cerebellar component u_{imp} compensates for whatever fraction of the vestibular signal entering the error is not already cancelled by the brainstem component $-\alpha_h \dot{x}_h$. In a third experiment involving an adapted VOR gain, it has been demonstrated that the VOR in the light is unaffected by changes in the VOR gain [37]. Figure 2 shows this experimental behavior with our model, where $\alpha_h = 2$ for $t \in [0, 15]$ and $\alpha_h = -1$ for $t \in [15, 30]$. It is clear from the left figure in Figure 2 that our model predicts that in steady-state, the VOR in the light is unaffected by changes in the VOR gain.

Next we consider neurological experiments with the VOR. An experiment reported in [30] demonstrated that the depth of firing rate of the output of the cerebellum increases with the frequency of sinusoidal head rotation while the subject fixates on a stationary target. In this case, $r = 0$ and $x_h = a_h \sin(\beta_h t)$. Considering the error model (6), the cerebellum must reject a disturbance signal with the form $-(1 - \alpha_h)\dot{x}_h - \widetilde{K}_x x_h$. In particular, the term $\dot{x}_h = a_h \beta_h \cos(\beta_h t)$ is proportional to β_h. Figure 3 shows the simulation results for $a_h = 15$, $\beta_h = 0.1$Hz for $t \in [0, 20]$; $\beta_h = 0.2$Hz for $t \in [20, 40]$; and $\beta_h = 0.5$Hz for $t \in [40, 60]$. We see in the right figure that the amplitude of u_{imp} increases as the frequency of the head rotation increases.

Finally, we consider lesion experiments with the VOR. A number of researchers have studied the VOR in the situation when the cerebellum is disabled either due to disease or cerebellectomy [58]. We illustrate this effect for *VOR cancellation*, in which the eyes must track a head fixed target; that is, the target position is mechanically coupled to the head position by

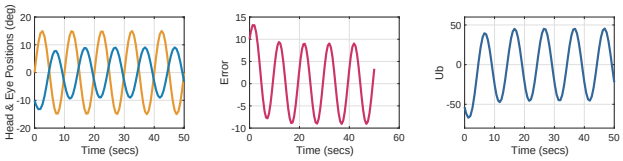

Fig. 4: VOR cancellation with the cerebellum disabled. From left to right, the head (yellow) and eye (blue) angles, the retinal error e, and the brainstem component u_b. The head movement is no longer suppressed.

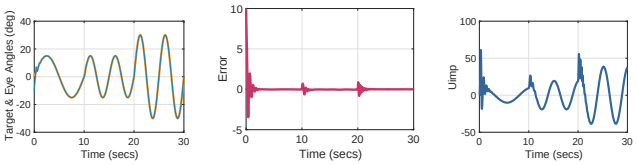

Fig. 5: Smooth pursuit of a sinusoidal target. The signals are the same as in Figure 3.

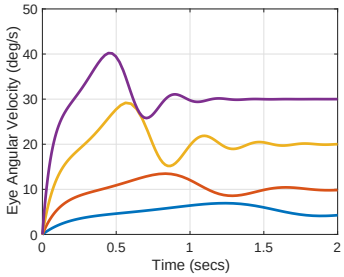

Fig. 6: Smooth pursuit of a ramp target with velocity $v = 5, 10, 20, 30$ (blue, red, yellow, purple).

an experimental apparatus so that $r(t) = x_h(t)$. Simulation results are shown in Figure 4 with $u_c = 0$ to disable the cerebellum. We observe in the left figure that the subject is no longer able to suppress the VOR - the blue curve shows that the eye position is not stabilized, despite a head-fixed target. This result corroborates many experimental findings [58].

In a second lesion experiment, a careful study of the effects of disabling the neural integrator on the VOR, OKR, gazing holding, and smooth pursuit appeared in [6]. In our model, disabling the neural integrator corresponds to removing the observer (11a) and setting $u_b = -\alpha_h \dot{x}_h$. For experiments conducted in total darkness, also $u_c = 0$. Therefore, in darkness the eye evolves according to dynamics $\dot{x} = -K_x x - \alpha_h \dot{x}_h$. Comparing with the normal eye dynamics in darkness: $\dot{x} = -\widetilde{K}_x x - \alpha_h \dot{x}_h$, we notice the change is in the constant $\widetilde{K}_x = 0.05 K_x \ll K_x$, where $\widetilde{K}_x$ was selected to approximate the known time constant of the combined oculomotor plant and neural integrator. For instance, for gaze holding with the head stationary, the eye drifts back to center with the time constant of the oculomotor plant. If the head angular velocity is a constant $\dot{x}_h = v$, then the eye position converges exponentially to $\overline{x} = -\alpha_h v / K_x$, rather than approximately tracking a ramp (with a very slow exponential decay). This is the behavior recovered in experiments [6]: a step of constant head velocity in total darkness evokes a step change in eye position, not in eye velocity.

Gaze Fixation: The purpose of the *gaze fixation* or *gaze holding system* is to stabilize the gaze on a stationary object. Gaze holding has been described as a distributed brain function, involving the oculomotor plant, the brainstem, and the cerebellum, and consisting of three time constants [14], [27]. The first time constant may be measured in darkness with the eye in an eccentric position at lights out, in an animal whose NPH has been lesioned [6]. With the head stationary, $u_b = 0$. Also $u_c = 0$ because the cerebellum (flocculus) is inactive in darkness. Then the eye evolves according to the dynamics $\dot{x} = -K_x x$, so the first time constant of gaze holding is $\tau_x = 1/K_x$, the time constant of the oculomotor plant itself. The second time constant is measured in normal (un-lesioned) subjects with the lights out. Then $u_b = \alpha_x \hat{x}$ and $u_c = 0$. Assuming $\hat{x}(t) \simeq x(t)$, the eye evolves according to dynamics $\dot{x} = -\widetilde{K}_x x$, so the second time constant of gaze holding is $\tilde{\tau}_x := 1/\widetilde{K}_x$, the time constant of the combined oculomotor plant and neural integrator. Finally, the third time constant is measured in the light while the subject fixates on a stationary target at an eccentric position. That is, $r \neq 0$ is constant and $x_h = 0$. Assuming that $\hat{x}(t) \simeq x(t)$, the error dynamics (6) take the form

$$\dot{e} = -\widetilde{K}_x e - u_c + \widetilde{K}_x r \,. \tag{14}$$

We see that to make the error go to zero it is necessary that $u_{imp} \simeq \widetilde{K}_x r$. Then the eye will evolve according to the dynamics $\dot{x} = -\widetilde{K}_x (x - r) + K_e e$. In particular, the steady-state value of x is r, so our model predicts an infinite time constant for gaze holding in the light. In practice, this time constant is closer to 25s, potentially depending on the subject's fatigue. Note that our model does not consider the effect on the time constants of remembered targets.

Finally, our model predicts that because the cerebellar component u_{imp} must cancel a disturbance $\widetilde{K}_x r$ for gazing holding, the output of the PCs will be proportional to the eye position. This behavior is observed experimentally in many studies [40].

Smooth Pursuit: The purpose of the *smooth pursuit system* is to keep a moving object centered on the fovea. Experiments with the smooth pursuit system may be categorized, analogously with the VOR, as behavioral, neurological, and lesion experiments. Here we discuss three behavioral experiments; see [4] for further results.

Figure 5 depicts smooth pursuit with our model for a sinusoidal target $r(t) = a_h \sin(\beta_h t)$, with $a_h = 15$, $\beta_h = 0.1$Hz for $t \in [0, 10]$ and $\beta_h = 0.2$Hz for $t \in [10, 20]$. We see that the cerebellar output u_{imp} is strongly modulated during tracking of a sinusoidal target, as observed experimentally [29]. Figure 6 depicts the transient response of our model for smooth pursuit of a ramp target $r(t) = vt$ with $v = 5, 10, 20, 30$. This transient response matches that reported in Figure 3 in [46].

In a series of experiments researchers explored the difference between *target stopping* and *target blanking*. In target stopping, a target with a ramp position is abruptly stopped. It is demonstrated experimentally that during target stopping, the oculomotor system switches from smooth pursuit to gaze fixation [33], [46]. In target blanking the target is blanked

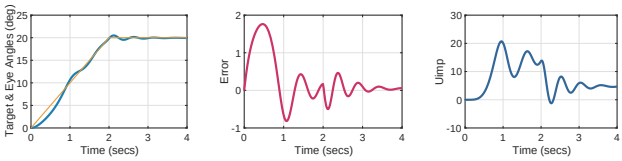

Fig. 7: Smooth pursuit with target stopping at $t = 2$s. From left to right, the eye angle (blue), the retinal error e, and the cerebellar component u_{imp}.

out or occluded, so that it is no longer visible. It is shown experimentally that with target blanking the eye continues to track for some time [7], [8]. Figure 7 depicts target stopping, in which $r(t) = 10t$ for $t \in [0, 2]$, and $r(t) = 20^\circ$ for $t \geq 2$. We observe that the error decays to zero with an exponential envelope after target stopping, as expected for the gaze fixation system. Target blanking is interpreted in our model to be the same as the *error clamp experiment* in which the smooth pursuit system continues to track for some time; see [4].

Remark 6.1: A well-known feature of the smooth pursuit system is that its tracking capability improves as the target motion becomes more predictable [1]. For example, humans are capable of perfect tracking of a single sinusoid or a ramp signal, while tracking multiple sinusoids is degraded [56]. For this reason, we have selected $q = 2$. Further experimentation is needed to confirm the value of q. The effect of an overmodeled (q too large) or undermodeled (q too small) exosystem has been investigated in [34], [35]. The extent to which these theoretical guarantees are applicable in a biological context requires further investigation. ◁

VII. Discussion

A mapping between brain projections and signals in our model is as follows; see [5]. The retinal error signal e descends from the visual cortex and is utilized in our model in three forms: as the projection from the IO to the CF input in (11c); as a visual MF input u_s; and again as a visual signal u_s in the MVN. Note that u_s may be distinct in the MVN v.s. the MFs; here it is the same signal only because of the mathematical parsimony of the adaptive internal model design [48]. Next, the projection from the PCs to the MVN corresponds to the signal u_{imp}. From the MVN this signal then projects to the MF input of the cerebellum and to the MNs. The direct projection from the vestibular system to the MVN and thence to the MNs is modeled by $\alpha_h \dot{x}_h$. The eye position signal $\alpha_x \hat{x}$ nominally corresponds to the projection from the NPH to the MNs; however, we do not make precise statements about its location as the neural substrate of the NPH is still under investigation [9], [16], [17]. As a final note, the MF inputs to the flocculus have been classified as visual, vestibular, and eye movement MFs [29]. In our model u_{imp} carries an estimate of all persistent disturbances acting on the retinal error, so this signal alone may account for the mixture of signals observed on the MF inputs of the cerebellum.

While we have not provided a detailed mapping to cell types in the MVN, our model may be amenable to such a mapping. For example, consider the EH neurons, a class of FTNs thought to be involved in long-term adaptation of the VOR gain [47]. These cells receive inputs from the PCs and the vestibular system; that is, $u_{eh} = u_{imp} + \alpha_{eh}\dot{x}_h$. During steady-state smooth pursuit with passive head rotation, our model predicts $u_{imp} \simeq \dot{r} + \widetilde{K}_x r - (1 - \alpha_h)\dot{x}_h - \widetilde{K}_x x_h$. Since $x(t) \simeq r(t) - x_h(t)$, this becomes $u_{imp} \simeq \dot{x} + \widetilde{K}_x x + \alpha_h \dot{x}_h$. Therefore, our model predicts $u_{eh} \simeq \dot{x} + \widetilde{K}_x x + (\alpha_h + \alpha_{eh})\dot{x}_h$, which is the formula obtained experimentally in [47, Fig. 14].

The neural circuit in [10] differs from our control architecture in two primary ways: (i) they assume a pure head velocity signal arrives at the MF inputs of the cerebellum; (ii) they assume the full motor command u is an MF input whereas we only use u_c. First, our model does not included a pure head velocity MF input. Not only are there no primary afferents [13], but all secondary afferents in the MVN carry other signals as well [45]. Additionally, the resting rate of vestibular only MF inputs does not match that of vestibular nerve fibers, whereas they have resting rates comparable to vestibular only neurons in the MVN [26], [31]. Finally, the smooth pursuit system, which relies in the cerebellum, is fully functional without any vestibular signal [54].

Second, our model does not make use of the projection from the NPH to the flocculus, presumed to provide an efference copy of the motor command u as an MF input, as doing so leads to inconsistencies with lesion experiments. If the NPH (but not the MVN) is lesioned, it is known that the VOR and smooth pursuit systems are still functional, showing minor changes in their transient responses [6], [20], [23]. It is also known that smooth pursuit is abolished after ablation of the flocculus [58]. If we assumed the projection from the NPH to the flocculus were u, we would arrive at a paradox that the smooth pursuit system can still function without an MF input to the cerebellum when the NPH is lesioned. In contrast, after lesioning the MVN, the VOR, the OKR, gaze holding, and smooth pursuit are all disabled or strongly modified, consistent with the idea that damage to the MVN effectively disables the flocculus [6].

The previous discussion reveals an apparent variability in the interpretion of the MF inputs in different models. Interestingly, this variability is mirrored in the variants of adaptive internal models in the control literature - as a deeper understanding of the MF inputs emerges, control theorists may respond in kind with alternative adaptive internal model designs. For example, an alternative design replaces (11b) by a minimal order observer:

$$\dot{\hat{w}} = F\hat{w} + Gu_c + (FG + G\widetilde{K}_x)e\,. \tag{15}$$

The benefit of this design is that it separates the rate of adaptation from stability of e, thereby obviating the need for high gain feedback (indeed our use of high gain feedback is not motivated by any biological considerations). On the other hand, (15) requires a more careful match up of system parameters, an assumption that must be justified in a biological context. For this reason we have elected to use (11b) here.

VIII. Conclusions

We have presented a model of the oculomotor system that incorporates a model of the cerebellum based on the

internal model principle of control theory. Our interpretation of cerebellar function contrasts with the prevailing view in neuroscience that the cerebellum provides adaptive internal models of the *systems* it regulates. While adaptive internal models of signals v.s. systems may appear superficially to be similar, the mathematical and conceptual consequences of the distinction are important.

Here we have focused on one module of the cerebellum: the floccular complex. Our future work will examine other modules such as the nodulus/uvula. Also, we require a control theoretic framework to explain long term adaptation, where the cerebellum will play the role of a *teacher* for the brainstem.

REFERENCES

[1] A.T. Bahill and J. McDonald. Smooth pursuit eye movements in response to predictable target motions. *Vision Research*. Vo. 23, No. 12, pp. 1573–1583, 1983.

[2] G. Blohm, M. Missal, and P. Lefevre. Direct evidence for a position input to the smooth pursuit system. *Journal of Neurophysiology*. Vol. 94, pp. 712-721, 2005.

[3] M.E. Broucke. Adaptive internal models: explaining the oculomotor system and the cerebellum. *arXiv:1901.01309 [q-bio.NC]*. January, 2019.

[4] M.E. Broucke. Model of the oculomotor system based on adaptive internal models. *IFAC World Congress*. July, 2020.

[5] U. Buttner and J. Bttner-Ennever. Present concepts of oculomotor organization. *Prog. Brain Research*. Vol. 151, pp. 1-42, 2006.

[6] S. Cannon and D. Robinson. Loss of the neural integrator of the oculomotor system from brain stem lesions in monkey. *J. Neurophysiology*. Vol. 57, No. 5, pp. 1383-1409, May 1987.

[7] N. Cerminara, R. Apps, and D. Marple-Horvat. An internal model of a moving visual target in the lateral cerebellum. *J. Physiology*. vol. 587, no. 2, pp. 429-442, 2009.

[8] M. Churchland, I. Chou, and S. Lisberger. Evidence for object permanence in the smooth-pursuit eye movements of monkeys. *J. Neurophysiology*. No. 90, pp. 2205-2218, 2003.

[9] A. Dale and K. Cullen. Local population synchrony and the encoding of eye position in the primate neural integrator. *J. Neuroscience*. Vol. 35, No. 10, pp. 4287-4295, March 2015.

[10] P. Dean, J. Porrill, and J. Stone. Decorrelation control by the cerebellum achieves oculomotor plant compensation in simulated vestibulo-ocular reflex. *Proc. R. Soc. Lond. B.* Vol. 269, pp. 1895-1904, 2002.

[11] B.A. Francis and W.M. Wonham. The internal model principle of control theory. *Automatica*. Vol. 12, pp. 457–465, 1976.

[12] H. Galiana and J. Outerbridge. A bilaternal model for central neural pathways in vestibuloocular reflex. *Journal of Neurophysiology*. Vol. 51, no. 2, pp. 210–241, February 1984.

[13] N.M. Gerrits, A.H. Epema, A.van Linge, and E. Dalm. The primary vestibulocerebellar projection in the rabbit: absence of primary afferents in the flocculus. *Neuroscience Letters*. Vol. 105, pp. 27-33, 1989.

[14] S. Glasauer. Cerebellar contribution to saccades and gaze holding. *Annals New York Academy of Sciences*. pp. 206-209, 2003.

[15] A. Gonshor and G. Melvill Jones. Extreme vestibulo-ocular adaptation induced by prolonged optical reversal of vision. *J. Physiology*. No. 256, pp. 381-414, 1976.

[16] A. Green, Y. Hirata, H. Galiana, and S. Highstein. Localizing sites for plasticity in the vestibular system. In: Highstein S.M., Fay R.R., Popper A.N. (eds) *The Vestibular System*. Vol. 19. Springer, 2004.

[17] A. Green, H. Meng, and D. Angelaki. A reevaluation of the inverse dynamic model for eye movements. *J. Neuroscience*. Vol. 27, no. 6, pp. 1346–1355, February 2007.

[18] B. Guthrie, J. Porter, and D. Sparks. Corollary discharge provides accurate eye position information to the oculomotor system. *Science*. Vol. 221, pp. 1193-1195, September 1983.

[19] C. Kassardjian, Y. Tan, J. Chung J, R. Heskin, M. Peterson, and D. Broussard. The site of a motor memory shifts with consolidation. *J. Neuroscience*. Vol. 25, Issue 35, pp. 7979-7985, 2005.

[20] C.R. Kaneko. Eye movement deficits after ibotenic acid lesions of the nucleus prepositus hypoglossi in monkeys, II: Pursuit, vestibular, and optokinetic responses. *J. Neurophysiology*. Vol. 81, pp. 668 - 681, 1999.

[21] M. Kawato. Internal models for motor control and trajectory planning. *Current Opinion in Neurobiology*. Vol. 9, No. 6, pp. 718-727, December 1999.

[22] M. Kawato and H. Gomi. A computational model of four regions of the cerebellum based on feedback-error learning. *Biological Cybernetics*. Vol. 68, pp. 95-103, 1992.

[23] S.-H. Kim, D. Zee, S. du Lac, H. Kim. J.-S. Kim. Nucleus prepositus hypoglossi lesions produce a unique ocular motor syndrome. *American Academy of Neurology*. Vol. 87, November 2016.

[24] G. Kim, J. Laurens, T. Yakusheva, and P. Blazquez. The macaque cerebellar flocculus outputs a forward model of eye movements. *Front. Integr. Neurosci.* 13:12, April 2019.

[25] R. Krauzlis, M. Basso, and R. Wurtz. Shared motor error for multiple eye movements. *Science*. No. 276, pp. 1693-1695, 1997.

[26] T. Langer, A. Fuchs, C. Scudder, and M. Chubb. Afferents to the flocculus of the cerebellum in the rhesus macaque as revealed by retrograde transport of horseradish peroxidase. *J. Comparative Neurology*. Vol. 235, pp. 1-25, 1985.

[27] J. Leigh and D. Zee. *The Neurology of Eye Movements*. Vol. 5, Oxford University Press, 2015.

[28] S. Lisberger. Neural basis for motor learning in the vestibuloocular reflex of primates. III. Computational and behavioral analysis of the sites of learning. *J. Neurophysiology*. Vol. 72, No. 2, August 1994.

[29] S. Lisberger. Internal models of eye movement in the floccular complex of the monkey cerebellum. *Neuroscience*. Vol. 162, No. 3, pp. 763–776, September, 2009.

[30] S. Lisberger and A. Fuchs. Role of primate flocculus during rapid behavioral modification of vestibuloocular reflex. I. Purkinje cell activity during visually guided horizontal smooth-pursuit eye movements and passive head rotation. *J. Neurophysiology*. Vol. 41, no. 3, pp. 733–763, May 1978.

[31] S. Lisberger and A. Fuchs. Role of primate flocculus during rapid behavioral modification of vestibuloocular reflex. II. Mossy fiber firing patterns during horizontal head rotation and eye movement. *J. Neurophysiology*. Vol. 41, no. 3, pp. 764–777, May 1978.

[32] S. Lisberger and T. Pavelko. Vestibular signals carried by pathways subserving plasticity of the vestibulo-ocular reflex in monkeys. *J. Neuroscience*. No. 6, Vol. 2, pp. 346-354, February 1986.

[33] A. Luebke and D. Robinson. Transition dynamics between pursuit and fixation suggest different systems. *Vision Research*. Vol. 28, No. 8, pp. 941-946, 1988.

[34] R. Marino and P. Tomei. An adaptive learning regulator for uncertain minimum phase systems with undermodeled unknown exosystems. *Automatica*. No. 47, pp. 739–747, 2011.

[35] R. Marino and P. Tomei. Disturbance cancellation for linear systems by adaptive internal models. *Automatica*. No. 49, pp. 1494–1500, 2013.

[36] R.C. Miall and D.M. Wolpert. Forward models for physiological motor control. *Neural Networks*. Vol. 9, No. 8, pp. 1265–1279, 1996.

[37] F. Miles and B. Eighmy. Long-term adaptive changes in primate vestibuloocular reflex. I. Behavioral observations. *J. Neurophysiology*. Vol. 43, No. 5, May 1980.

[38] V. O. Nikiforov. Adaptive servocompensation of input disturbances. *IFAC World Congress*. pp. 5114-5119, 1996.

[39] V. O. Nikiforov. Observers of external deterministic disturbances II. objects with unknown parameters. *Automation and Remote Control*. Vol. 65, No. 11, pp. 1724-1732, 2004.

[40] H. Noda and D. Suzuki. The role of the flocculus of the monkey in fixation and smooth pursuit eye movements. *J Physiology*. No. 294, pp. 335-348, 1979.

[41] J. Pola. Models of the saccadic and smooth pursuit systems. In: G. Hung, K. Ciuffreda (eds). *Models of the Visual System*. Springer, 2002.

[42] J. Porrill, P. Dean, and J. Stone. Recurrent cerebellar architecture solves the motor-error problem. *Proc. Royal Soc. Lond. B*. No. 271, pp. 789-796, 2004.

[43] R. Ramanchandran and S. Lisberger. Neural substrate of modified and unmodified pathways for learning in monkey vestibuloocular reflex. *J. Neurophysiology*. No. 100, pp. 1868–1878, 2008.

[44] D. A. Robinson. The effect of cerebellectomy on the cat's vestibulo-ocular integrator. *Brain Research*. Vol. 71, pp. 195–207, 1974.

[45] D.A. Robinson. The use of control systems analysis in the neurophysiology of eye movements. *Ann. Rev. Neuroscience*. No. 4, pp. 463–503, 1981.

[46] D.A. Robinson, J.L. Gordon, and S.E. Gordon. A model of the smooth pursuit eye movement system. *Biological Cybernetics*. No. 55, pp. 43-57, 1986.

[47] J. Roy and K. Cullen. Brain Stem Pursuit Pathways: Dissociating Visual, Vestibular, and Proprioceptive Inputs During Combined Eye-Head Gaze Tracking. *J. Neurophysiology*. Vol. 90, pp. 271-290, 2003.

[48] A. Serrani and A. Isidori. Semiglobal nonlinear output regulation with adaptive internal model. *IEEE Conference on Decision and Control*. pp. 1649-1654, December, 2000.

[49] A. Serrani, A. Isidori, L. Marconi. Semiglobal nonlinear output regulation with adaptive internal model. *IEEE Transactions on Automatic Control*. Vol. 46, No. 8, pp. 1178-1194, 2001.

[50] F. Shutoh, M. Ohki, H. Kitazawa, S. Itohara, and S. Nagao. Memory trace of motor learning shifts transsynaptically from cerebellar cortex to nuclei for consolidation. *Neuroscience*. No. 139, pp. 767-777, 2006.

[51] A. Skavenski and D. Robinson. Role of abducens neurons in vestibuloocular reflex. *J. Neurophysiology*. No. 36, pp. 724–738, 1973.

[52] P. Sylvestre and K. E. Cullen. Quantitative analysis of abducens neuron discharge dynamics during saccadic and slow eye movements. *J. Neurophysiology*. Vol. 82, issue 5, pp. 2612–2632, November 1999.

[53] P. Tomei. Multi-sinusoidal disturbance rejection for discrete-time uncertain stable systems. *Automatica*. No. 79, pp. 144-151, 2017.

[54] J. Waterston, G. Barnes, M. Grealy, and L. Luxon. Coordination of eye and head movements during smooth pursuit in patients with vestibular failure. *J. Neurology, Neurosurgery, and Psychiatry*. Vol. 55, pp. 1125-1131, 1992.

[55] D. Wolpert, R.C. Miall, and M. Kawato. Internal models in the cerebellum. *Trends in Cognitive Sciences*. Vol. 2, no. 9, pp. 338–347, September 1998.

[56] H.J. Wyatt and J. Pola. Predictive behavior of optokinetic eye movements. *Exp. Brain Res.* No. 73, pp. 615-626, 1988.

[57] C. Yilmaz and H. Basturk. Output feedback control for unknown LTI systems driven by unknown periodic disturbances *Automatica*. Vol. 99, pp. 112-119, 2019.

[58] D. Zee, A. Yamazaki, P. Butler, and G. Gucer. Effects of ablation of flocculus and paraflocculus on eye movements in primate. *J. Neurophysiology*. Vol. 46, No. 4, pp. 878–899, October 1981.

[59] X. Zhang and H. Wakamatsu. A unified adaptive oculomotor control model. *International Journal of Adaptive Control and Signal Processing*. No. 15, pp. 697-713, 2001.